Thin Solid Films, *114* (1984) 295–309
PREPARATION AND CHARACTERIZATION

LOW PRESSURE CHEMICAL VAPOUR DEPOSITION AT QUASI-HIGH FLOW

JISK HOLLEMAN AND JAN MIDDELHOEK
Department of Electrical Engineering, Twente University of Technology, P.O. Box 217, 7500 AE Enschede (The Netherlands)
(Received July 14, 1983; accepted February 9, 1984)

A new chemical vapour deposition (CVD) technique is presented. It is especially advantageous for the deposition of compound materials. The technique improves the uniformity and reproducibility of the deposition. The economical use of gaseous reactants is improved by a factor varying between 5 and 20. This is important in the case of expensive metal–organic CVD methods. The method consists in the manifold repetition of the following sequence: evacuation, filling and deposition in a horizontal tube reactor. The filling time of 50 ms is short compared with the deposition period of 1 s.

The advantages of the method are demonstrated with results for the deposition of undoped, phosphorus-doped and boron-doped silicon and SiO_2.

1. INTRODUCTION

Chemical vapour deposition (CVD) in a horizontal reactor with continuous flow at low pressure still has some shortcomings for the deposition of compound materials and also for large batches of substrates. The concentration of active reactants decreases in the axial direction of the tube depending on the various reaction rates. The application of a temperature gradient is one means of restoring constant deposition for a single reaction. A high flow of the reactants forms another approach but at the expense of very uneconomical use of the gases.

In this paper the results achieved with a new technique will be shown. For this purpose the horizontal reactor tube was provided at both ends with fast electromechanical valves controlled by a microprocessor. The tube is first evacuated and then filled in a very short time with the desired mixture of the gaseous reactants from a buffer volume. The deposition then takes place and the sequence of evacuation, filling and deposition is repeated.

2. THEORY

The deposition of a solid A onto a surface from a gaseous reactant AB can be represented by

$$AB(g) + \text{surface} \rightarrow A(s) + B(g) \qquad (I)$$

0040-6090/84/$3.00
© Elsevier Sequoia/Printed in The Netherlands

A general expression for the growth rate is

$$r = (kC)^n \tag{1}$$

The deposition rate as a function of the position x in a horizontal tube reaction with continuous flow can be approximated by

$$r_x = r_0\left[1 - \frac{n\{1+(\varepsilon-1)C_0 C_{g0}^{-1}\}A_x r_0}{\mathrm{MF}} - n\frac{\Delta p}{p}\right] \tag{2}$$

(Appendix A). The pressure drop Δp cannot always be neglected and increases with increasing mass flow.

From eqn. (2) it can be seen that the mass flow of the reactants must be much greater than

$$n\left\{1+(\varepsilon-1)\frac{C_0}{C_{g0}}\right\}A_0 r_x$$

to obtain equal growth for all wafers. High mass flows, however, lead to poor efficiency of the reactants and to an increasing pressure drop between $x = 0$ and $x = x$. Only a small percentage of the gas is used. In order to overcome the problem of poor efficiency we studied an intermittent method. The reactor is filled within 50 ms with the reacting gas, followed by a reaction period without flow. Then about 80% of the gaseous reactants in the hot zone is used for deposition. During the filling period the mass flow is very high: velocities as high as 3000–6000 cm s^{-1} in the annular area can be calculated. If we ignore any concentration decay of the reactants during filling, the growth rate during the reaction period can be given by

$$r_t = r_{t0}\left\{1 - \frac{(1-n)Ar_{t0}t}{C_{t0}V}\right\}^{n/(1-n)} \tag{3}$$

(see Appendix A).

3. EXPERIMENTAL DETAILS

Figure 1 is a schematic diagram of the reactor. The filling of a buffer volume is controlled by mass flowmeters. The reactor pressure is controlled by the time that the inlet valves are opened and the flow into the buffer volume. In a steady state the amount leaving the buffer volume per cycle equals the flow (in cubic centimetres per minute) divided by the number of cycles per minute. Fast magnetic valves are mounted between the buffer volume and the reactor inlet and also at the reactor outlet. The pump is a 1 m^3 min^{-1} rotary pump. The three-zone furnace has a 30 cm constant temperature zone. The quartz tube of the reactor has a diameter of 7 cm. Deposition is carried out onto 2 in silicon wafers. For polycrystalline silicon (poly-Si) deposition the substrates were first coated with Si_3N_4. Uncoated silicon substrates were used for SiO_2 deposition. A quartz carrier 25 cm long was placed directly at the entrance of the constant zone. In some cases another carrier was placed upstream of the first. Undiluted SiH_4 was used. PH_3 and B_2H_6 were diluted to 0.2% in argon. Several sequences for a deposition cycle are possible (Fig. 2).

Undoped poly-Si was deposited according to sequences I and II. Doped poly-Si was deposited according to sequences I, II and IV. In the case of sequence IV PH_3 or

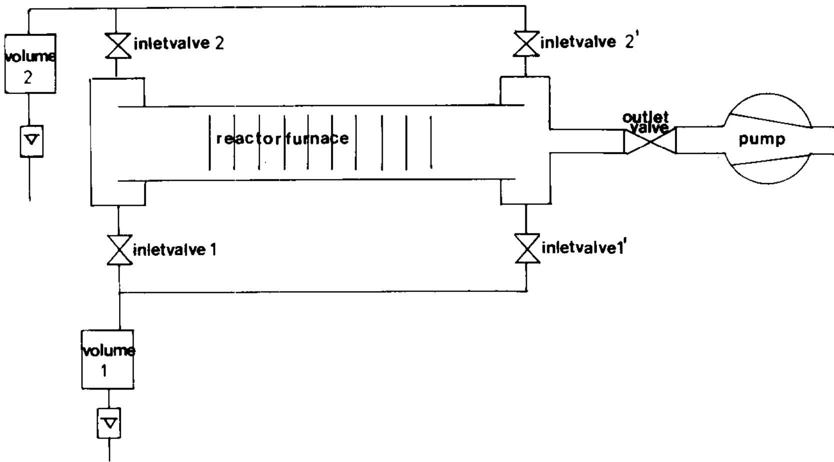

Fig. 1. Schematic diagram of the reactor system.

B_2H_6 was injected via buffer volume 2 and SiH_4 via volume 1. Sequence V was used for the deposition of SiO_2 from SiH_4 and O_2.

4. FILLING THE REACTOR TUBE

First we studied how fast the reactor tube is filled. Figure 3 shows the pressure changes during a cycle. The pressure was measured at the inlet using a capacitance manometer and a storage oscilloscope. A pressure overshoot at the inlet was found, except for hydrogen. No difference was found whether the reactor tube was loaded with wafers or not. We found that the pressure overshoot is considerably less when the reactor is at room temperature. The overshoot can be explained by assuming a certain resistance caused by the occurrence of a pressure wave during the warming of the cold gas as it enters the hot zone. The much higher heat conductance coefficient of hydrogen and its lower viscosity could explain the absence of the overshoot in this case. After stabilization a pressure rise can be observed with SiH_4 because of the conversion of one SiH_4 molecule into two hydrogen molecules. We can draw the following conclusions from Fig. 3.

(1) The reactor is filled in 50 ms.

(2) Stabilization including heating of the gas occurs within 100 ms.

The initial pressure after filling as well as the pressure change during a cycle can be valuable tools for studying the kinetics of the reaction. In our case, however, the reactor volume in the cold part was too large compared with the volume in the hot region to draw conclusions on the role of adsorption, the order of the reaction etc.

5. UNDOPED POLYCRYSTALLINE SILICON

In order to estimate the suitable conditions for the intermittent flow, we first studied the deposition of undoped silicon from SiH_4 under continuous flow. The layer growth was determined by the weight increase of the wafers. In the case of continuous flow at a reactor temperature of 630 °C and an SiH_4 pressure of 10 Pa, a

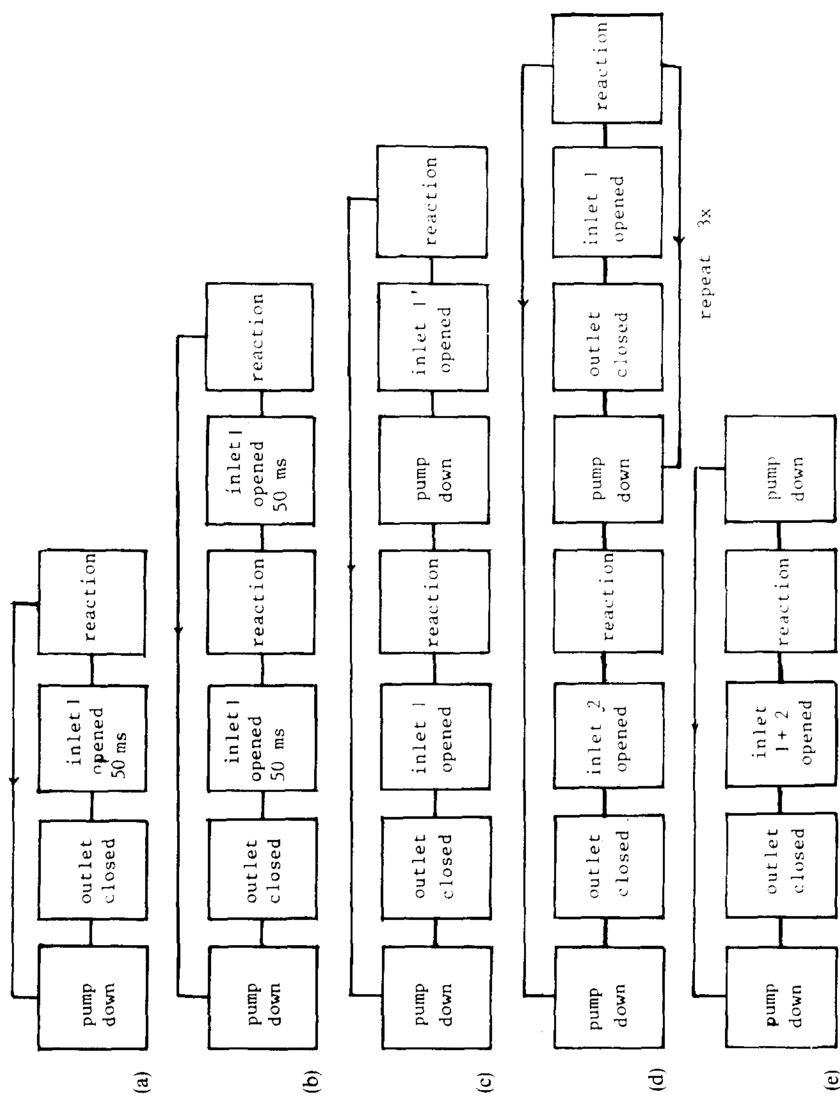

Fig. 2. Sequences of pumpdown and refill: (a) sequence I; (b) sequence II; (c) sequence III; (d) sequence IV; (e) sequence V.

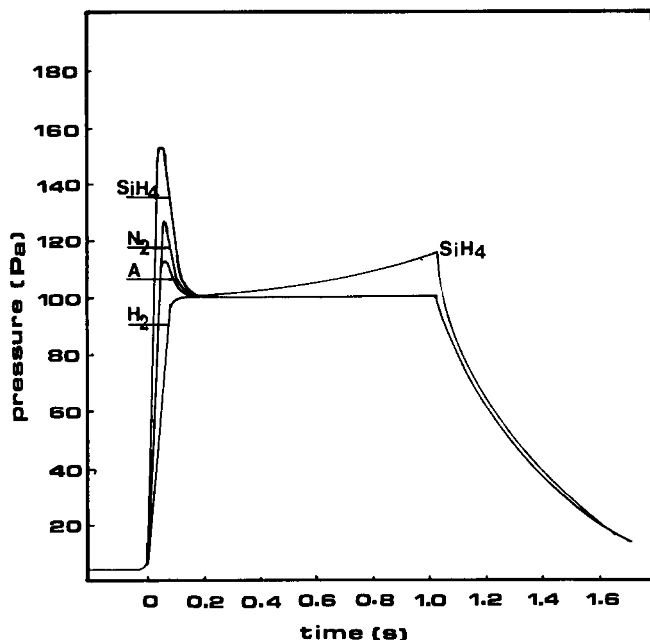

Fig. 3. Pressure change during a cycle (flow into the volume, 60 $cm^3 min^{-1}$). The cycle is as follows: pumpdown, 1 s; injection; non-flow period, 1 s.

deposition rate of 0.2 nm s^{-1} was found. This corresponds to a growth rate of 1×10^{15} atoms $cm^{-2} s^{-1}$. An SiH_4 pressure of 10 Pa at 630 °C corresponds to 8.8×10^{14} SiH_4 molecules cm^{-3}. The distance between the wafer was 1 cm and $A/V = 1.7 cm^{-1}$.

Now we can calculate with the help of eqn. (3) that a nearly full depletion of the reactant is achieved in about 1 s at 630 °C when $n = 0.5$ [1]. Increasing the reaction period or the temperature does not result in the deposition of a larger amount per cycle as a full depletion will already be reached within 1 s at 630 °C.

Figure 4 shows some results for undoped silicon deposition. The higher growth rate for the first and last wafers in two series can be explained by assuming an extra supply of reactant by diffusion from the volume outside the batch of wafers where the value of A/V is lower. Placing several dummy wafers at both ends of the batch and applying a small negative temperature gradient from the middle of the zone towards the ends of the batch as in the series represented by × and △ easily prevents the higher growth rate towards the ends of the batch.

Table I shows the results for the middle wafer of the batch. It is clear that by increasing the pump speed the pumpdown time can be decreased and so the total number of cycles per unit time can be increased; hence the total layer thickness deposited in 1 h can be increased. This requires a large pump.

6. BORON-DOPED POLYCRYSTALLINE SILICON

Figure 5 shows the results for the deposition of boron-doped silicon. A uniform deposition rate is obtained. The resistivity was measured after an anneal for 40 min

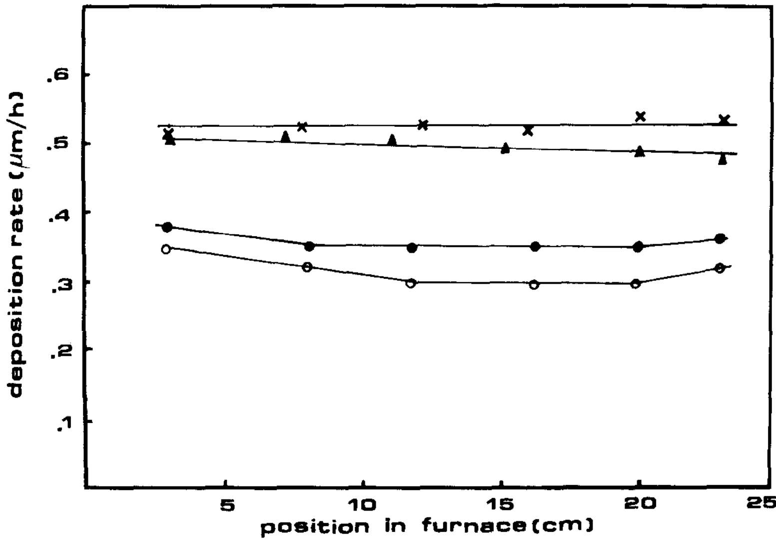

Fig. 4. Undoped poly-Si deposition at 650 °C: ○, sequence I (SiH_4 flow, 4.2 cm^3 min^{-1}; N_2 flow, 37.2 cm^3 min^{-1}; pumpdown time, 1 s; reaction time, 2 s; total pressure per cycle, 100 Pa; SiH_4 pressure, 10 Pa); ●, sequence I (SiH_4 flow, 6.3 cm^3 min^{-1}; N_2 flow, 56.0 cm^3 min^{-1}; pumpdown time, 1 s; reaction time, 1 s; total pressure per cycle, 100 Pa; SiH_4 pressure, 10 Pa); ×, sequence II (SiH_4 flow, 13.8 cm^3 min^{-1}; N_2 flow, 112.5 cm^3 min^{-1}; pumpdown time, 1 s; reaction time, 0.5 plus 0.5 s); ▲, sequence I (SiH_4 flow, 10 cm^3 min^{-1}; N_2 flow, 10 cm^3 min^{-1}; pumpdown time, 2 s; reaction time, 1 s).

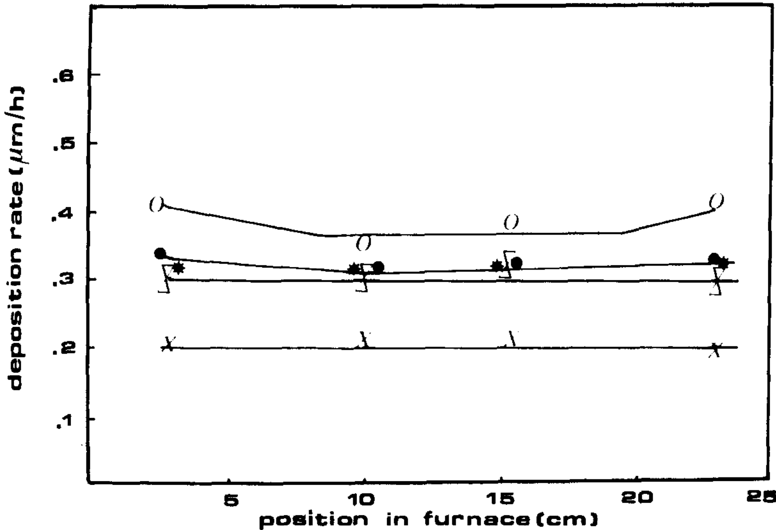

Fig. 5. Boron-doped poly-Si deposition rate at 650 °C *vs.* position in the furnace (position 0 corresponds to 15 cm before the middle of the furnace): ●, sequence I (SiH_4 flow, 10 cm^3 min^{-1}; B_2H_6 flow, 100 cm^3 min^{-1}; pumpdown time, 2 s; reaction time, 1 s); ○, sequence I (SiH_4 flow, 10 cm^3 min^{-1}; B_2H_6 flow, 100 cm^3 min^{-1}; pumpdown time, 1 s; reaction time, 2 s); △, sequence I (SiH_4 flow, 10 cm^3 min^{-1}; B_2H_6 flow, 150 cm^3 min^{-1}; pumpdown time, 2 s; reaction time, 1 s); ▽, sequence I (SiH_4 flow, 10 cm^3 min^{-1}; B_2H_6 flow, 100 cm^3 min^{-1}; pumpdown time, 1 s; reaction time, 0.5 s); ✱, sequence III (SiH_4 flow, 10 cm^3 min^{-1}; B_2H_6 flow, 50 cm^3 min^{-1}; N_2 flow, 50 cm^3 min^{-1}; pumpdown time, 2 s; reaction time, 1 s). For clarity △, ▽ and ✱ are represented by a single curve.

TABLE I

RESULTS FOR THE DEPOSITION OF UNDOPED SILICON

Symbol in Fig. 4	*SiH_4 flow* ($cm^3\ min^{-1}$)	*N_2 flow* ($cm^3\ min^{-1}$)	P_{tot} (Pa)	P_{SiH_4} (Pa)	*Reaction time* (s)	*Pumpdown time* (s)	*Thickness deposited per hour* (nm)	*Thickness deposited per cycle* (nm)	*Sequence*	*Temperature* (°C)
○	4.2	37.2	100	10	2	1	300	0.250	I	630
●	6.5	56.0	100	10	1	1	300	0.200	I	630
×	13.8	112.5	100–200	10	0.5 + 0.5	1	530	0.295	II	630
△	10.0	10.0	50	25	1	2	510	0.433	I	655

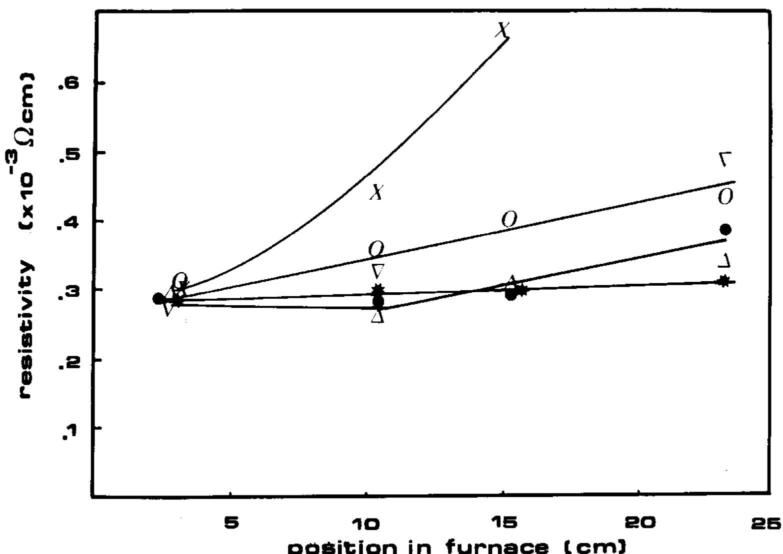

Fig. 6. Resistivity of boron-doped poly-Si after a 40 min nitrogen anneal at 1050 °C *vs.* the position in the furnace. Symbols as for Fig. 5; ○, ▽ and ●, △ each represented by a single curve.

in nitrogen at 1050 °C. It can be seen from Fig. 6 that the resistivity increases with increasing distance along the furnace. This indicates that B_2H_6 decomposes appreciably during the filling period. However, it can also be seen that a longer reaction time improves the batch uniformity of the resistivity. This is in contradiction to the proposed explanation.

Sequentially injecting the gas in the front and the rear of the reactor markedly improves the batch uniformity. The resistivity of about 2.8×10^{-3} Ω cm, found in all experiments for the front wafers, corresponds to boron-saturated poly-Si.

7. PHOSPHORUS-DOPED SILICON

Figures 7 and 8 show the results for phosphorus-doped silicon. The resistivity was measured after a nitrogen anneal for 40 min at 1050 °C. Good thickness and resistivity uniformity can be achieved. However, acceptable resistivities correspond to a low deposition rate. An improvement in the deposited thickness by a factor of 2 is possible with a shorter pumpdown time using a larger pump, resulting in more cycles per unit of time.

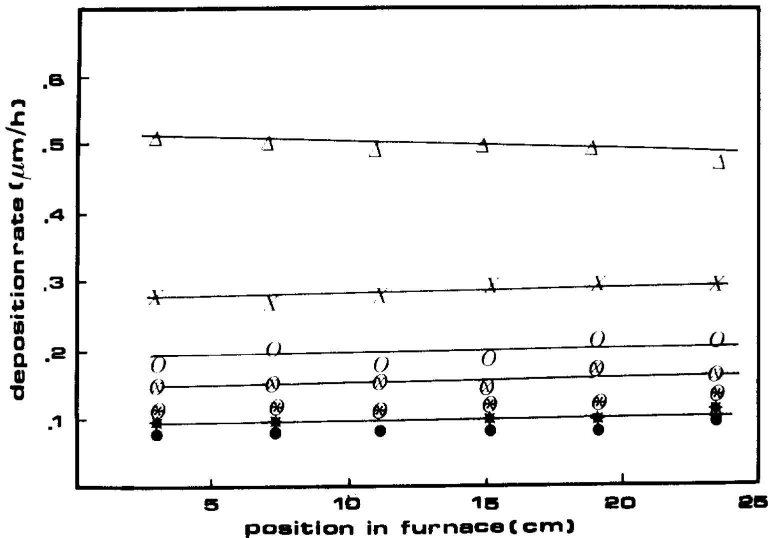

Fig. 7. Deposition rate *vs.* position in the furnace for phosphorus-doped poly-Si (position 0 corresponds to 15 cm before the middle of the furnace): sequence I. The symbols have the following meanings.

Symbol	*Temperature* (°C)	*SiH_4 flow* ($cm^3\,min^{-1}$)	*PH_3 flow (0.2% in Ar)* ($cm^3\,min^{-1}$)	*Pumpdown time* (s)	*Reaction time* (s)
△	655	10	—	2	1
●	655	10	35	2	1
⊗	655	10	5	2	1
○	675	10	5	2	1
✱	700	5	10	2	6
⊛	700	10	20	2	2
×	700	10	5	2	1

For clarity ⊛, ✱ and ● are represented by a single curve.

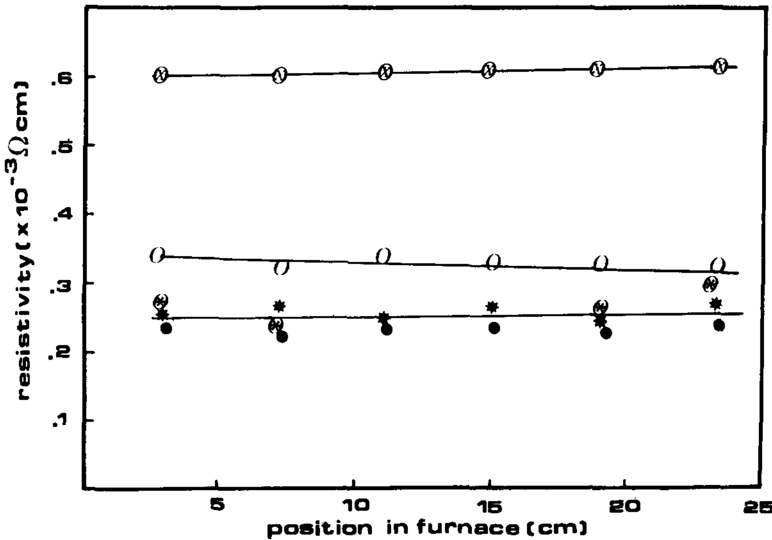

Fig. 8. Resistivity of phosphorus-doped poly-Si after a 40 min nitrogen anneal at 1050 °C *vs.* position in the furnace. Symbols and other details as for Fig. 7.

8. PHOSPHORUS- AND BORON-DOPED POLYCRYSTALLINE SILICON DEPOSITION ACCORDING TO SEQUENCE IV

This method allows boron or phosphorus and silicon to be deposited sequentially. It was expected that higher deposition rates could be obtained for phosphorus-doped poly-Si because the PH_3 at surface sites[2] or step sites can decompose independently of SiH_4. However, this was not the case. Figure 9 shows the results for boron-doped, phosphorus-doped and undoped silicon. The reaction time was 1 s for PH_3 or B_2H_6 decomposition as well as for SiH_4 decomposition, the pumpdown time after PH_3 or B_2H_6 reaction was 4 s and that after SiH_4 reaction was 1 s. Undoped and boron-doped poly-Si depositions were carried out at 630 °C. The deposition rate of phosphorus-doped silicon at 630 °C was hardly measurable, but at 700 °C a measurable rate was found. The concentration of PH_3 per cycle after injection was about 1×10^{13} PH_3 molecules cm^{-3}. Considering that there are 1.3×10^{15} surface sites per square centimetre and 2 cm^2 of surface per cubic centimetre, the marked decrease in the silicon deposition rate cannot be explained by assuming that the surface sites become saturated with PH_3 as was proposed elsewhere[2].

However, if we assume that PH_3 fills step sites, the density of which is much lower than that of surface sites, then it must be assumed that the PH_3 still remains on the surface during pumpdown. This would finally lead to a saturation of step sites with PH_3 on subsequent refills. However, the growth rate was found to depend on the amount of PH_3 supplied per cycle which excludes the model in which step sites are covered with PH_3. A model presented earlier[3] in which the surface Fermi potential is assumed to be responsible for the reduced deposition rate of phosphorus-doped poly-Si and the enhanced deposition rate of boron-doped silicon is therefore more probable. For boron-doped silicon deposition it can be seen

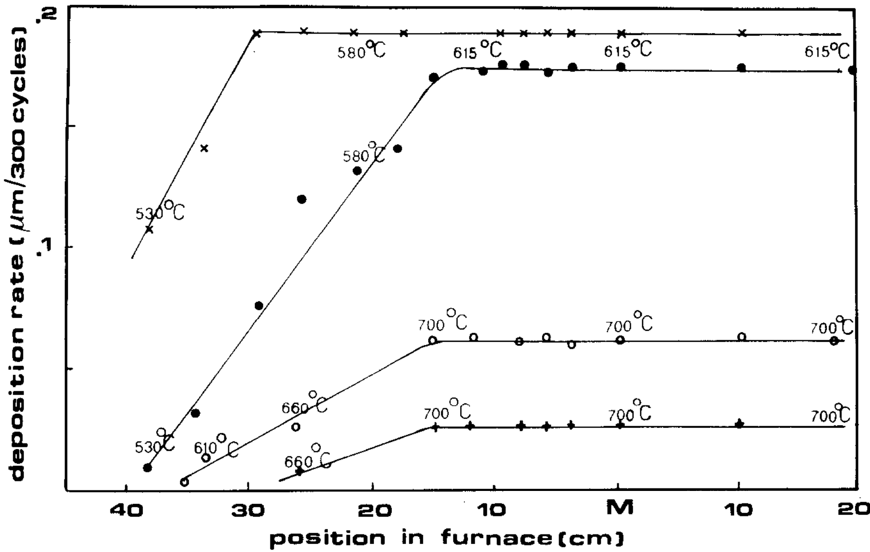

Fig. 9. Deposition rates of undoped, boron-doped and phosphorus-doped poly-Si according to sequence IV (position M corresponds to the middle of the furnace). The symbols have the following meanings.

Symbol	*Temperature* (°C)	*SiH_4 flow* ($cm^3\ min^{-1}$)	*PH_3 flow* ($cm^3\ min^{-1}$)	*B_2H_6 flow* ($cm^3\ min^{-1}$)	*N_2 flow* ($cm^3\ min^{-1}$)
×	615	3	—	100	—
●	615	3	—	—	100
○	700	3	25	—	—
+	700	3	50	—	—

that within the reaction time full depletion of the reactants is achieved at temperatures higher than 550 °C.

9. LOW TEMPERATURE OXIDE FROM SiH_4 AND OXYGEN

Initial experiments were carried out at 400 °C and the same problems as presented by Rosler[4] were found. A lower deposition rate was found at that part of the wafer which is in contact with the quartz boat, and the SiO_2 layer is thicker at the edges of the wafer. Backing the 2 in wafer with a $2\frac{1}{4}$ in wafer placed at a distance of 1 mm showed additional improvement in the uniformity at the edges of the wafer. Uniformities of 3% could be achieved except for the point of contact with the quartz boat. Figure 10 shows the results of SiO_2 deposition. The SiH_4 partial pressure per cycle could be as high as 30 Pa before the deposited layers showed a hazy appearance. This is about six times higher than the value reported by Rosler[4]. The initial increase in the deposition rate with distance along the furnace may be a result of the temperature rise. The decrease for higher temperatures must be attributed to the occurrence of depletion during filling and to an extra deposit due to the fact that unreacted SiH_4 plus oxygen from the cold inlet parts of the reactor passes the wafers in the hot zone during pumpdown. An increase in the reaction time from 1 to 2 s did not yield a greater deposition per cycle in the hot zone. Decreasing the reaction time

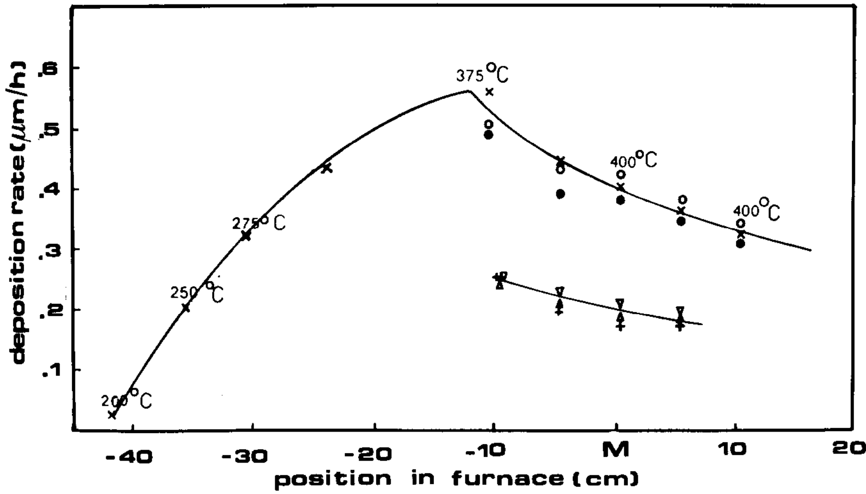

Fig. 10. Low temperature oxide deposition rate *vs.* position in the furnace. The symbols have the following meanings.

Symbol	*SiH_4 flow* ($cm^3\ min^{-1}$)	*O_2 flow* ($cm^3\ min^{-1}$)	*Pumpdown time* (s)	*Reaction time* (s)
×	10	10	2	1
○	10	10	1	2
●	10	10	2.5	0.5
+	5	5	2	1
△	5	10	2	1
▽	5	20	2	1

from 1 to 0.5 s gave only a 10% reduction in the deposition rate. This means that also during filling and stabilization, which takes about 0.1 s, a considerable amount of depletion takes place. We propose three methods to prevent wafer-to-wafer non-uniformity for SiO_2 deposition: (1) a decrease in the deposition temperature to about 300 °C; (2) sequential injection from the front and the back; (3) pumpdown from both sides of the reactor.

It can be seen from Fig. 10 that below 300 °C no full depletion is achieved within the reaction time of 1 s. At 200 °C only 20% of the deposition rate at 400 °C is obtained. Nevertheless the non-uniformity at the point of contact in the quartz boat and the edges of the wafers remains. In the case of a continuous flow reactor it has been shown[5] for silicon deposition that the occurrence of edge non-uniformities or "bull's-eyes" above a critical concentration of SiH_4 is due to the polymerization of SiH_4 in the gas phase. As the polymers have a lower diffusion coefficient they deposit mainly onto the outer rim of the wafers when they diffuse from the annular area into the cavity formed by two wafers. In our case, however, the cavity is filled with the reacting gas within 50 ms which is very short compared with the total time needed to achieve full depletion at 200 °C. So the concentration of reactant inside the cavity is the same everywhere at the onset of reaction and, as only a little of the reactant is used during the reaction period of 1 s, it is not very likely that a diffusion barrier will dominate the growth.

A probable explanation is that a gas phase reaction is rate controlling, and as the surface per unit volume is much larger at the quartz boat this leads to a lower deposition rate there and to a higher deposition rate at the edges where the surface per unit volume is lower. Edge inhomogeneities can be overcome by creating a larger surface in the vicinity of the edge, for example by backing the wafers with a larger wafer. Hitchman and Kane[6] have arrived at similar conclusions for oxygen-doped poly-Si.

10. CONCLUSIONS

Low pressure CVD at quasi-high flow improves the economics of the reactants' use. Good within-wafer uniformity and batch uniformity can be achieved for boron-doped, phosphorus-doped and undoped poly-Si.

SiO_2 deposition gives good within-wafer uniformity, although some reactor improvements are still necessary to achieve good batch uniformity. Compound materials can be deposited by codeposition but the method also allows the separate deposition of the compounding materials layer by layer which can be advantageous in the deposition of III–V compounds.

The method also permits additional conclusions to be drawn on the kinetics of low pressure CVD. We have suggested, in the case of phosphorus-doped poly-Si that growth is reduced because of the surface Fermi potential rather than the blocking of surface sites by adsorbed PH_3. Observation of the change in pressure during a cycle can also give additional information. We also showed that within-wafer non-uniformities are not caused by diffusion limitations in the case of SiO_2 deposition.

REFERENCES

1 J. Holleman and A. A. J. Aarnink, *Proc. 8th Int. Conf. on Chemical Vapour Deposition, Paris, September 1981*, Electrochemical Society, Pennington, NJ, 1981.
2 H. Kurokawa, *J. Electrochem. Soc.*, *129* (1982) 2620.
3 Y. Yasuda, K. Hirabayastic and T. Moriya, *Proc. 5th Conf. on Solid-State Devices, Tokyo, 1973*, in *Jpn. J. Appl. Phys., Suppl.*, *43* (1974) 400.
4 R. S. Rosler, *Solid State Technol.*, *20* (April 1977) 63.
5 C. H. J. van den Brekel and L. J. M. Bollen, *J. Cryst. Growth*, *54* (1981) 310.
6 M. L. Hitchman and J. Kane, *J. Cryst. Growth*, *55* (1981) 485.

APPENDIX A

A1. Growth rate at quasi-high flow

If we ignore the degree of depletion during filling we can calculate the growth per cycle at constant reactor volume as follows:

$$r = (kC)^n \tag{A1}$$

$$r = -\frac{V}{A}\frac{\mathrm{d}C}{\mathrm{d}t} \tag{A2}$$

$$\frac{1}{C^n}\frac{\mathrm{d}C}{\mathrm{d}t} = -k^n\frac{A}{V} \tag{A3}$$

$$C_t^{\,1-n} - C_{t0}^{\,1-n} = -k^n\frac{A}{V}(1-n)t \tag{A4}$$

$$C_t^n = \left\{C_{t0}^{1-n} - (1-n)\frac{A}{V}k^n t\right\}^{n/(1-n)} \tag{A5}$$

$$r_t = r_{t0}\left\{1-(1-n)\frac{A}{V}\frac{r_{t0}}{C_{t0}}t\right\}^{n/(1-n)} \tag{A6}$$

For $n = 1$ we get

$$\frac{dC}{dt} = -\frac{A}{V}kC \tag{A7}$$

$$C_t = C_{t0}\exp\left(-t\frac{A}{V}k\right) \tag{A8}$$

$$r_t = r_{t0}\exp\left(-t\frac{A}{V}k\right) \tag{A9}$$

For $t < (V/A)k$

$$r_t = r_{t0}\left(1-\frac{Ar_{t0}t}{VC_{t0}}\right) \tag{A10}$$

In the case of continuous flow we can derive an equation similar to eqns. (A6) and (A10), although including the effect of self-dilution and including the pressure drop across the batch. The flux of reactant is governed both by diffusion and by convection and is given by

$$F = -D\frac{dC}{dx} + vC \tag{A11}$$

For a typical case with $p_g = 50$ Pa, $p_{SiH_4} = 10$ Pa, $T = 900$ K, a total flow of 500 $cm^3 min^{-1}$, $O = 40 cm^2$, assuming a 50% SiH_4 concentration decay over a length of 50 cm and using

$$D = 0.1\left(\frac{T}{300}\right)^2 \frac{10^5}{p} \qquad cm^2 s^{-1}$$

we get $D(dC/dx) = 1.8 \times 10^{16}$ molecules $cm^{-2} s^{-1}$ and $vC = 4 \times 10^{17}$ molecules $cm^{-2} s^{-1}$. So in most practical low pressure chemical vapour deposition cases $vC > D(dC/dx)$ and eqn. (A11) becomes

$$F = vC \tag{A12}$$

The decrease in the flux of the reactant gas with x is given by

$$\frac{dF}{dx} = -\frac{A'}{O}r \tag{A13}$$

The total flux is given by

$$F_g = C_g v \tag{A14}$$

and the change in total flux by

$$\frac{dF_g}{dx} = +\frac{A'}{O}(\varepsilon-1)r \tag{A15}$$

The total gas concentration at x is given by

$$C_g = C_{g0}\left(1-\frac{\Delta p}{p}\right) \tag{A16}$$

From eqns. (A12) and (A13) we can derive

$$v\frac{dC}{dx}+C\frac{dv}{dx} = -\frac{A'}{O}r \tag{A17}$$

If the reactant gas is greatly diluted in a carrier gas and if the pressure drop is negligible we may consider the velocity changes in the length direction to be negligible. Equation (A17) then becomes

$$v\frac{dC}{dx} = -\frac{A'}{O}r \tag{A18}$$

Now using eqn. (A1) we get

$$\frac{dC}{C^n} = -\frac{A'k^n\,dx}{vO} \tag{A19}$$

and in a similar way as for eqns. (A2)–(A6) and with

$$vOC = \mathrm{MF} \tag{A20}$$

we get

$$r = r_0\left\{1-\frac{(1-n)A_x r_0}{\mathrm{MF}}\right\}^{n/(1-n)} \tag{A21}$$

However, if the reactant gas is not greatly diluted in a carrier gas and $\varepsilon > 1$ or if the pressure drop is considerable then the term $C(dv/dx)$ in eqn. (A17) cannot be ignored. From eqns. (A14) and (A15) we can obtain

$$C\frac{dv}{dx} = +\frac{CA'r}{C_gO}(\varepsilon-1)-\frac{Cv}{C_g}\frac{dC_g}{dx} \tag{A22}$$

Substituting eqn. (A22) into eqn. (A17) and with $C/C_g \approx C_0/C_{g0}$ we get

$$\frac{dC}{dx} = -\frac{A'r}{Ov}-\frac{CA'r}{C_gOv}(\varepsilon-1)+\frac{Cv}{C_g}\frac{dC_g}{dx} \tag{A23}$$

From eqn. (A26) we can arrive in a similar way as with eqns. (A2)–(A6) at

$$r = r_0\left[1-\frac{(1-n)\{1+(\varepsilon-1)(C_0/C_{g0})\}A_x r_0}{\mathrm{MF}}-(1-n)\frac{\Delta p}{p}\right]^{n/(1-n)} \tag{A24}$$

For $n = 0.5$ and also for other values of n provided that the degree of conversion is not too great we may write

$$r = r_0\left[1-\frac{n\{1+(\varepsilon-1)(C_0/C_{g0})\}A_x r_0}{\mathrm{MF}}-n\frac{\Delta p}{p}\right] \tag{A25}$$

It should be kept in mind that eqn. (A25) is no longer valid when diffusion becomes more important than convection. In that case we cannot obtain an analytical expression similar to eqn. (A25). A numerical solution of the problem will then be necessary as was presented by Kuiper *et al.*[A1] and Jensen and Graves[A2].

References for Appendix A

A1 A. E. T. Kuiper, C. H. J. van den Brekel, J. de Groot and G. W. Veldkamp, *J. Electrochem. Soc.*, *129* (1982) 2288.
A2 K. F. Jensen and D. B. Graves, *J. Electrochem. Soc.*, *130* (1983) 1950.

APPENDIX B: NOMENCLATURE

A'	amount of surface area per unit length (cm)
A/V	amount of surface area per unit volume (cm^{-1})
A_x	total surface area between $x = 0$ and $x = x$ (cm^2)
C	concentration of reactant (molecules cm^{-3})
C_g	total concentration of gas (molecules cm^{-3})
F	flux of reactant (molecules cm^{-2} s^{-1})
F_g	total flux of gas (molecules cm^{-2} s^{-1})
k	reaction rate constant
MF	mass flow of reactants (molecules s^{-1})
n	order of reaction
O	annular area between substrate and reactor wall (cm^2)
p	total pressure (Pa)
Δp	pressure drop between $x = 0$ and $x = x$ (Pa)
r	growth rate (atoms cm^{-2} s^{-1})
t	time
v	velocity of gas (cm s^{-1})
V	volume (cm^3)
x	position in the furnace (cm)
ε	number of gaseous molecules formed by the decomposition of one molecule of reactant

Subscripts

g	refers to total gas
g0	refers to total gas at inlet of constant temperature zone
t	at time $t = t$ (s)
$t0$	at time $t = 0$
x	refers to the position in the furnace
0	refers to the inlet of the constant temperature zone